Microbes and Infectious Diseases 2024; 5(2): 632-646

Microbes and Infectious Diseases

Journal homepage: https://mid.journals.ekb.eg/

Original article

Piroxicam repurposing approach as an anti-virulence agent against methicillin resistant *Staphylococcus aureus* clinical isolates

Ingy El-Soudany[1]*, Maged A. El Sawy[2], Rasha Emad[3], Nancy Attia[4]

1- *Microbiology and Immunology department, Pharos University in Alexandria, Alexandria, Egypt.*
2- *Pharmaceutical Chemistry department, Pharos University in Alexandria, Alexandria, Egypt.*
3- *Alexandria Main University Hospital, Alexandria University, Alexandria, Egypt.*
4- *Microbiology department, Medical Research Institute, Alexandria University, Alexandria, Egypt.*

ARTICLE INFO

Article history:
Received 19 February 2024
Received in revised form 14 March 2024
Accepted 14 March 2024

Keywords:
MRSA
Anti-virulence
Piroxicam
Biofilm formation
agr system

ABSTRACT

Background: Methicillin resistant *Staphylococcus aureus* (MRSA) is a major pathogen that causes infections in a wide range due to its high virulence. Anti-virulence therapy is one of several strategies proposed to counteract antimicrobial resistance. FDA-approved drugs repurposing as antibacterial and anti-virulence agents is a promising and rapid approach. The study aimed to evaluate piroxicam effect, a repurposed drug, as anti-virulence agent against MRSA isolated from chronic infections. **Methods:** The minimum inhibitory concentration (MIC) of piroxicam against the MRSA isolates was estimated. The presence of various virulence factors including protease, hemolysin, staphyloxanthin and biofilm formation was assessed in the absence and presence of piroxicam at ½ MIC. The detection of *agr* genes was performed using PCR for *agr* typing of the isolates. Molecular docking studies was performed to investigate whether piroxicam can bind to specific virulence proteins. **Results:** Piroxicam exhibited an MIC of 2.5mg/ml against all tested isolates. Piroxicam ½ MIC caused a significant reduction in protease activity (20-100% inhibition), hemolysin activity (20.7-97.2% inhibition) and staphyloxanthin production (1.17 -94.63% inhibition). In terms of biofilm formation, there was a significant inhibition ranging from 4.6-76.1%. The isolates were either type *agr1* (53.3%) or type *agr3* (46.7%). The anti-virulence effect of piroxicam was confirmed through *in-silico* docking, which demonstrated interactions between piroxicam and virulence proteins. **Conclusions:** Piroxicam has significant anti-virulence and anti-biofilm effects at sub-MIC against MRSA isolates. Therefore, it can be concluded that piroxicam can be used as an anti-virulence agent against MRSA infections.

Introduction

Staphylococcus aureus (*S. aureus*) is a Gram-positive opportunistic pathogen, causing both community- and hospital-acquired infections, resulting in substantial morbidity and mortality [1]. The emergence of methicillin-resistant *S. aureus* (MRSA) strains was due to the indiscriminate use of antibiotics and they can cause both acute and chronic infections. Those infections include skin abscesses, osteomyelitis, pneumonia, infections

DOI: 10.21608/MID.2024.271311.1805
* *Corresponding author:* Ingy El-Soudany
E-mail address: *ingy.elsoudany@pua.edu.eg*

linked to medical devices, bacteremia, and infective endocarditis [2].

MRSA strains express a multitude of virulence determinants that enable surfaces adherence, escaping, or even invading the immune system. These virulence factors include extracellular enzymes that aid the penetration of host cells e.g. lipases, nucleases, proteases, staphylokinase and hyaluronidase as well as coagulase. Furthermore, they secrete toxins, such as hemolysins, superantigens as toxic shock syndrome toxin, and Panton Valentine leukocidin, enterotoxins and exfoliative toxins [3]. Staphyloxanthin is another virulence factor that helps *S. aureus* escaping the host immune defense [4].

Surface-associated virulence factors like adhesins are responsible for bacterial attachment to the extracellular matrix and biofilm formation, which can be formed at the sites of the implanted medical devices. One of the clinical significances of biofilm is the increased antibiotic resistance [5].

The quorum sensing (QS) system accessory gene regulator (*agr)* operon can control many virulence determinants expression. It is regulated in a cell density-dependent manner through producing and sensing of auto-inducing peptides (AIPs). In *S. aureus*, there are four types of AIP autoinducers named; *agr1*, *agr2*, *agr3*, and *agr4* [6].

Bacterial virulence is a novel target that has strongly attracted research interest in the recent years. Anti-virulence drugs aim to disarm bacteria by reducing the production of virulence factors, without compromising its viability which may prevent the potential development of drug resistance [7].

Drug repurposing seems to be an excellent rapid strategy where the drugs are already FDA-approved. Recently, several studies displayed the repurposing of nonsteroidal anti-inflammatory drugs (NSAIDs) that exert some antibacterial and anti-biofilm activities against clinically important bacteria [4, 8].

Therefore, this study aimed to evaluate the effect of piroxicam, as a repurposed drug, against selected virulence factors such as staphyloxanthin, hemolysin, protease activity and biofilm formation in MRSA isolates obtained from various chronic infections.

Materials and methods

Bacterial isolates and antimicrobial resistance

Thirty MRSA clinical isolates obtained from patients with chronic infections are included in the current study. *S. aureus* ATCC 25923 standard strain was also included in the study from Microbiology Department, Medical Research Institute, Alexandria University. For initial identification of the isolates, conventional biochemical methods were applied [9], then bacterial identification was confirmed by Vitek-2 (bioMerieux, France).

For the detection of antibacterial susceptibility for all the included isolates, disc diffusion method was used. The discs used (Oxoid, London, UK) were, ampicillin (AMP, 10µg), cefoxitin (FOX, 30µg), levofloxacin (LEV, 5µg), ceftaroline (CPT, 30µg), tetracycline (TE, 30µg) and trimethoprim-sulfamethoxazole (SXT, 1.25\23.75µg), gentamicin (CN, 10µg) and azithromycin (AZT, 15µg) discs. The disc diffusion method and interpretation were conducted in accordance with recommendations of Clinical and Laboratory Standards Institute (CLSI), 2022 [10].

Minimum inhibitory concentration (MIC) of piroxicam against the MRSA isolates

MIC of piroxicam (Feldene® IM ampules 20 mg/ml Pfizer, Egypt) against MRSA isolates and *S. aureus* strain ATCC 25923 were determined using broth microdilution method [10]. For each isolate, the inoculum turbidity was adjusted to an optical density OD_{600} of 0.12–0.13, then diluted to obtain 5×10^5 CFU/ml as a final concentration. Each isolate then was examined against piroxicam - in microtiter plates- (in nutrient broth with twofold serial dilutions) at concentrations ranging from 10,000 to 19.5µg/ml. Each isolate was tested in duplicate where the average MIC was calculated. The concentration just below the MIC was considered the sub-MIC; ½ MIC used in further tests.

Phenotypic detection of some virulence factors and the effect of piroxicam ½ MIC

Assay of protease activity

Quantitative investigation of protease activity was estimated using the skimmed milk agar assay [11]. Briefly, Muller Hinton agar plates containing 1 % skimmed milk were prepared. Each isolate was cultured overnight in the presence and absence of piroxicam at ½ MIC, then 40µl of each isolate was inoculated in wells cut by a sterile cork-

borer (of 7 mm diameter). After incubation of the plates for 24 h at 37 °C, the halo-zone diameter was measured for each isolate under both conditions. The percentage decrease in the halo-zone diameter in the presence of piroxicam at ½ MIC was calculated as an indication of protease activity inhibition.

Hemolysin assay

Each isolate was cultured in TSB alone as a control and TSB containing piroxicam at ½ MIC till post-exponential phase at OD_{600} of 2.5, which corresponds to 1×10^9 CFUs/ml. Following centrifugation at 5500 rpm at 4°C, supernatant (100µl) were added to 1 ml of hemolysis buffer (0.145 mol/l NaCl plus 0.02 mol/l $CaCl_2$). Then adding 25µl of defibrinated rabbit blood to the mixture then incubation at 37°C for 15 min. Centrifugation at 5500 rpm at room temperature for 1 min will produce a supernatant containing the liberated hemoglobin. The absorbance of supernatant was measured at 543 nm using spectrophotometer Shimadzu UV 18000. The drug-free supernatant (control isolates) hemolytic activity was considered 100%. The hemolysis activity percentage in the presence of piroxicam was calculated [12]. The assay was performed in duplicates.

Staphyloxanthin assay

We performed the staphyloxanthin inhibition assay as previously outlined by Al-kazaz et al [13]. In brief, each isolate was incubated overnight, where the bacterial suspensions were then adjusted to 0.5 MacFarland Standard. Each isolate was subcultured on TSA plates (control plates) and then on TSA plates containing piroxicam ½ MIC. After 2 days of incubation at 37 °C, the bacterial colonies were collected and the surfaces of agar were rinsed with distilled water. Cells were collected after centrifugation of the suspensions at 6000 rpm for 15 min. Three ml 99% methanol were added to the cells' pellets. This mixture was then heated in a 55 °C water bath for 30 min. This was followed by 10 min of cooling and re-centrifugation at 6000 rpm for 15 min. The staphyloxanthin yellow pigment extracted was measured spectrophotometrically at 450 nm (Shimadzu UV 18000). The assay was performed in duplicates.

Biofilm forming capacity

The quantitative assay for biofilm forming capacity by the isolates and the standard strain was carried out according to the methodology stated by [14] with slight modifications. An overnight culture of the isolates in TSB was prepared where each isolate was cultured in absence and presence of ½ MIC piroxicam. The suspension turbidity was adjusted to 10^6 CFU/ml. In a microtiter plate wells the bacterial suspension of each isolate (200µl) was transferred and incubated at 37 °C for 48 h. A negative control only broth without bacterial isolates was included in the microtiter plate. The broth was gently discarded and then using phosphate buffer saline (PBS, pH 7.2) the wells were washed. The biofilm was fixed using 99% methanol (200µl for 20 minutes). Staining of the formed biofilm was performed using solution of 1% crystal violet for 15 min. After washing the excess dye, elution of the stain was done using 33% glacial acetic acid. The optical density was measured at 570 nm with ELISA plate reader (BioTek). The experiment was done in triplicates for each condition. The average optical density (OD) for each isolate was calculated and also the negative control average optical density (ODc). The interpretation of biofilm forming capacity was done according to Hassan et al., [15]. Moreover, the biofilm formation percentage inhibition by ½ MIC of piroxicam was calculated for each isolate using the formula stated by Lopes et al [16].

Detection of genes for *agr* typing by polymerase chain reaction (PCR)

DNA extraction of isolates was done using boiling method [17]. The four *agr* genes (*agr*1, *agr*2, *agr*3 and *agr*4) were detected by multiplex PCR (2 sets) using Veriti Thermal Cycler (Applied Biosystems). The utilized primers sequences are mentioned in **Supplementary table S1** [18]. In each run there was a negative control in which the DNA extract was replaced with water. The thermal profile applied was 95 °C for 3 min as initial denaturation step, afterward 35 cycles for denaturation at 95 °C for 15 s, then primer annealing at 55 °C for 15 s, then primer elongation step at 72 °C for 30 s. Then a final extension step at 72 °C for 5 min. Visualization of the amplicons took place through 1.8% agarose gel electrophoresis.

Molecular docking

We used molecular docking studies to explore piroxicam binding sites to *S. aureus* virulence proteins, including dehydrosqualene synthase, hemolysin, serine protease, sortase enzyme, IcaR, and AgrA LytTR. This will help better understanding of potential intermolecular

interactions while screening the possibility of a binding pattern that could be at the forefront of the piroxicam activation or inhibitory activities for these targets.

***In silico* study for piroxicam interactions with target proteins**

Computer-aided docking experiments have been executed the usage of Molecular Operating Environment software (MOE 2020.0802, Chemical Computing Group, Montreal, Canada). Consequently, the structure of dehydrosqualene synthase (2ZCQ), hemolysin (7AHL), serine protease (2VID), sortase enzyme (2KID), IcaR (3GEU), and AgrA LytTR (3BS1) were attained from the Protein Data Bank (PDB) and handled accordingly with the program MOE [19-24].

Docking procedure

The MOE-Site Finder was practiced to build up the active site of the receptor, while the MOE-Dock was hired to dock the ligands within this active site. The placement method running was the Triangle Matcher, with 15 preserved poses as parameters, and the scoring function used was London and GBV1/WAS dG. To courage the ideal docking pose and binding interactions, a thorough examination of each receptor-ligand complex was conducted. The selection of the best-docked complex, which is assumed to accurately represent the protein-ligand interactions, was based on factors such as the docking score, ligand alignment at the active site, and the retention of significant interactions. The graphical representations in the study were stemming using MOE version 2020.0802. In order to organize the process, unnecessary chains, water molecules, and any surfactants were removed from the models. Additionally, explicit hydrogen atoms were assimilated into the receptor complex structure, and partial charges were computed for accurate analysis. To ensure the accuracy of the molecular models, a structure preparation module requiring protonated 3D function was employed. The co-crystal ligand B65 was extracted from the protein (PBD ID 2ZCQ) and practiced as a reference compound for the subsequent validation study. Piroxicam, was made using the builder module of MOE, followed by the addition of hydrogens, calculation of partial charges, and energy minimization using force field MMFF94x.

Statistical analysis

The statistical analysis was managed in RStudio by R language (version R.4.2.3). Ggplot2, finalfit and Rstatix are the main used packages. Normality of data was determined by *Shapiro-Wilk* test and QQ plots. Count and percent presented categorical variables while median and interquartile range summarized continuous data. We tested not normal distributed data by Wilcoxon rank sum test. Statistical significance was considered at P-value $\leq$ 0.05.

Results

Bacterial isolates and antimicrobial resistance

The current study has included 30 MRSA clinical isolates and one standard strain ATCC 25923. All isolates were obtained from different chronic infections during a time period of 10 months. They were mainly wound swabs (20/30, 66.7 %) followed by osteomyelitis (7/30, 23.3%), and sputum (3/30, 10%) specimens.

All the isolates showed 100% resistance to both cefoxitin and ampicillin while all were completely susceptible to ceftaroline. Moreover, levels of resistance for azithromycin, tetracycline, cotrimoxazole, gentamicin, and levofloxacin were 43.3% (13 isolates), 40% (12 isolates), 40% (12 isolates), 36.7% (11 isolates), and 33.3% (10 isolates), respectively.

MIC of piroxicam against the MRSA isolates

Piroxicam showed MIC of 2.5mg/ml for all the investigated isolates and was 1.25 mg/ml for the ATCC 25923 strain. The sub-MIC (½ MIC) was selected to be used in the following phenotypic investigations (1.25mg/ml and 0.625mg/ml for the clinical isolates and the standard strain, respectively).

Phenotypic detection of some virulence factors and the effect of piroxicam ½ MIC

Inhibition of protease activity

Only 4 out of the 30 isolates did not show a halo zone on skimmed milk agar; indicating no protease activity. Piroxicam showed a significant reduction in the diameter of the halo zones produced by the isolates showing protease activity ($p < 0.00001$) **(Figure 1)**. The calculated percentage inhibition in protease activity ranged from 20 to 100%. The ATCC 25923 strain protease activity was completely inhibited (100%) when treated with piroxicam ½ MIC.

Inhibition of hemolysin activity

All the 30 MRSA isolates and the standard strain showed a hemolytic activity. There was a significant reduction in the hemolytic activity in the isolates in the presence of piroxicam unlike the control isolates (absence of piroxicam) ($p < 0.001$) **(Figure 1)**. The mean inhibition of hemolysin activity in the presence of piroxicam was 60.3%. In addition, piroxicam had an inhibitory effect on the hemolytic activity of the standard strain of 69.9%.

Reduction of staphyloxanthin production

All the clinical isolates and the standard strain produced staphyloxanthin pigment. This pigment production was significantly decreased when treated with piroxicam ½ MIC ($p<0.0001$) **(Figure 1)**. This was represented in a percentage inhibition ranging from 1.17 to 94.63% and 32.5 % for the standard strain.

Inhibition of biofilm formation

In the absence of piroxicam, 50% of isolates were strong biofilm formers while 33% and 17% of the isolates formed moderate and weak biofilm, respectively. On the other hand, no strong biofilm formation was observed upon using ½ MIC of piroxicam and the majority of isolates 83% became weak biofilm formers **(Figure 2)**. The OD of stain eluted from biofilm of isolates treated with piroxicam was significantly abolished ($p < 0.00001$) **(Figure 1)**. The biofilm percentage inhibition of the isolates ranged from 4.6 to 76.1%. The standard strain was a weak biofilm producer and remained the same in the presence of piroxicam, still showed a percentage inhibition of 5.5 %.

Detection of genes for *agr* typing by PCR

Neither *agr2* or *agr4* were present among the tested isolates. The *agr1* gene was detected among 16 (53.3%) isolates while *agr3* was present in 14 (46.7%). The piroxicam inhibitory action of staphyloxanthin was found significantly higher 73.6% (55.4-78.9%) among isolates of type *agr1* compared to isolates of *agr3* 45.5% (7.5-66.9%) (**Table 1**).

Molecular docking

Molecular docking showed that piroxicam can bind efficiently for all the tested proteins. The docking algorithm's validity was firmly established by re-docking the co-crystallized ligand B65 into the binding site for 2ZCQ. The initial poses captured from the Protein Data Bank (PDB) exhibited a root mean square deviation of 1.43Å and a docking score of -12.26 kcal/mol for 2ZCQ. These findings, presented in **Figure 3** and **Table 2**, demonstrated that the docking protocol had the capability to accurately predict docking poses for the compounds under investigation. It was noted that values below 1.5 or 2 Å were indicative of a successful and dependable docking protocol [25].

The optimal docked position of piroxicam within the active sites of the 2ZCQ, 3GEU, 2KID, 2VID, 7AHL, and 3BS1 enzymes corresponded the binding energy score (S) of -4.44, -4.87, -5.06, -4.87, -4.40, and -4.63 kcal/mol, respectively. Details of the interactions, including the type of non-covalent bonding interaction, binding distance, and residues involved in the interaction that activate the 3GEU receptor and inhibit the activities of other targets, were compiled in **Table 2** and shown in **Figures 3–5**.

Table 1. Percent of inhibition of different virulence factors and their association with type of agr system among *S. aureus* clinical isolates (N= 30)

N= 30	**Isolates with *agr1***, n= 16	**Isolates with *agr3***, n= 14	**p*-value
% Inhibition of hemolysin	51.9 (23.7-81.8)	64.3 (52.1-86.0)	0.298
% Inhibition of staphyloxanthin	73.6 (55.4-78.9)	45.5 (7.5-66.9)	**0.016**
% Inhibition of protease activity	41.7 (34.6-59.1)	42.3 (29.4-100.0)	0.883
% Inhibition of biofilm formation	61.4 (55.0-72.1)	73.9 (61.7-74.4)	0.279

Data is presented in median and interquartile range. *Wilcoxon test, bold p-value indicates statistically significant difference.

Table 2. The molecular docking results of B65 and piroxicam into 2ZCQ and molecular docking results of piroxicam into 3GEU, 2KID, 2VID, 7AHL and 3BS1

Ligand	Protein	Binding energy score (S) (Kcal/mol)	*RMSD	Binding distance (Å)	Type of binding interactions	Residues involved in the interaction
B65	2ZCQ	– 12.26	1.43	3.05 and 3.29	Hydrogen bonds	The Sulfonate oxygen with Arg 45
				3.25 and 3.26	Hydrogen bonds	The Sulfonate oxygen with Asn 168
				2.80	Hydrogen bond	The Phosphono oxygen with Gln 165
				3.66	Non-classical hydrogen bond	3-phenoxyphenyl with Leu 141
				2,25 and 2.51	Metal-coordination bonds	The Sulfonate oxygen with MG 452
				2.14 and 2.17	Metal-coordination bonds	The Phosphono oxygen with MG 453
Piroxicam	2ZCQ	– 4.44	___	3.26	hydrogen bond	The 1,1-dioxobenzothiazine with Arg 45
				2.83	hydrogen bond	The 1,1-dioxobenzothiazine with Asn 168
				2,24	Metal-coordination bonds	The 1,1-dioxobenzothiazine with MG 452
				2.31	Metal-coordination bonds	The 1,1-dioxobenzothiazine with MG 453
Piroxicam	3GEU	– 4.87	___	3.13	Hydrogen bond	1,1-dioxobenzothiazine with Arg 94
				3.27	Hydrogen bond	The 3-carboxamide oxygen with Asn 101
				3.55	Non-classical hydrogen bond	The pyridine ring with Ser 100
Piroxicam	2KID	– 5.06	___	2.94 and 3.13	hydrogen bonds	The 1,1-dioxobenzothiazine with His 120 and Arg 197
				4.74	Non classical hydrogen bond	The N-methyl benzothiazine with His 120
Piroxicam	2VID	– 4.87	___	3.21	Hydrogen bond	The carboxamide oxygen with Asn 127
				2.97	Hydrogen bond	The 4-hydroxy benzothiazine with Asn 127
Piroxicam	7AHL	– 4.40	___	3.33	Hydrogen bond	1,1-dioxobenzothiazine with Thr 155
				3.31	Hydrogen bond	The 3-carboxamide oxygen with Lys 154
Piroxicam	3BS1	– 4.63	___	3.38	Hydrogen bond	1,1-dioxobenzothiazine with His 169
				4.28	Non-classical hydrogen bond	The pyridine ring with Thr 166
				3.82	Non-classical hydrogen bond	Benzothiazine ring with His 169

*RMSD: root mean square deviation

Supplementary Table S1. Primers' sequences used in this study [18]**.**

Primer	**Nucleotide Sequence (5'–3')**	**Target**	**Amplicon size (bp)**
agr pan F	ATGCACATGGTGCACATGC		
agr1 R	GTCACAAGTACTATAAGCTGCGAT	***agr1***	439
agr2 R	GTATTACTAATTGAAAAGTGCCATAGC	***agr2***	572
agr3 R	CTGTTGAAAAAGTCAACTAAAAGCTC	***agr3***	406
agr4 R	CGATAATGCCGTAATACCCG	***agr4***	657

Figure 1. Violin plots showing inhibitory actions of piroxicam as anti-virulence agent on (A) Hemolysin production, (B) Staphyloxanthin production, (C) Protease activity, (D) Biofilm formation.

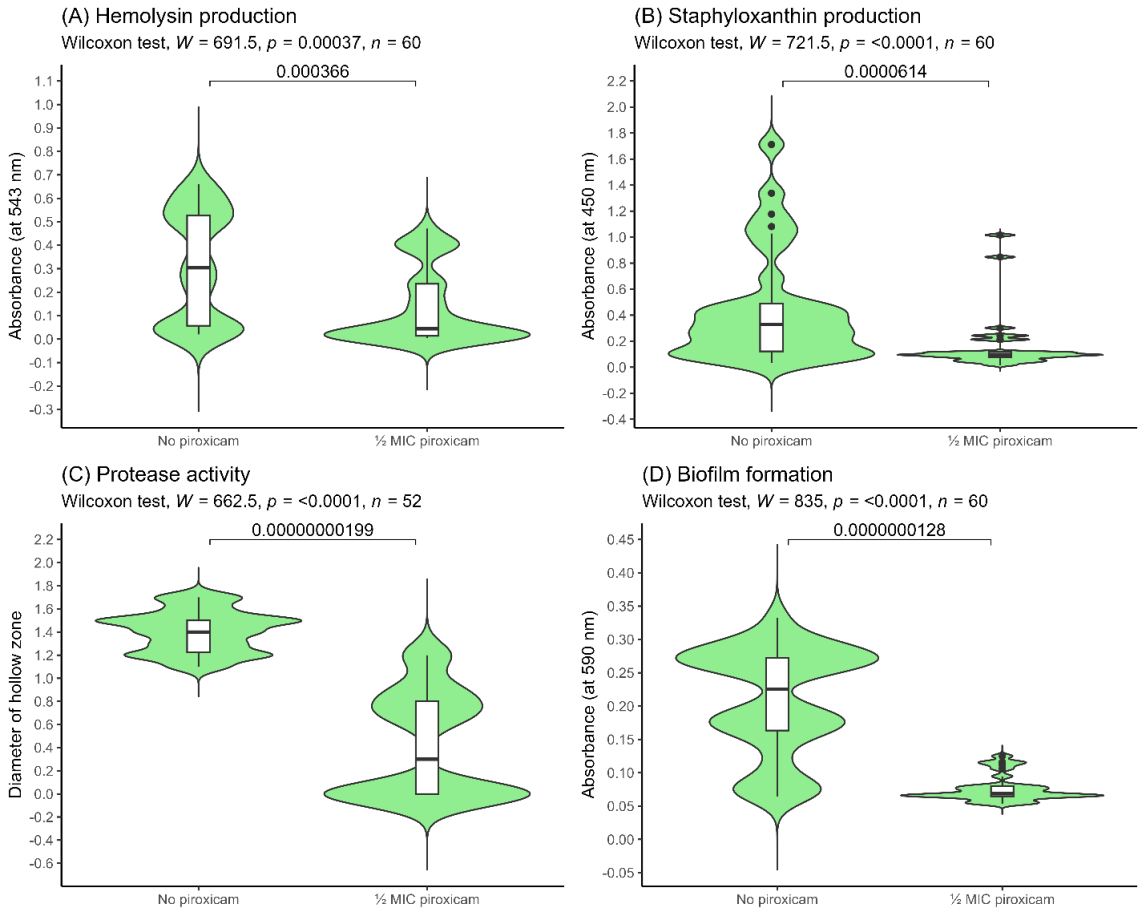

Figure 2. Biofilm strength in the absence and presence of ½ MIC piroxicam.

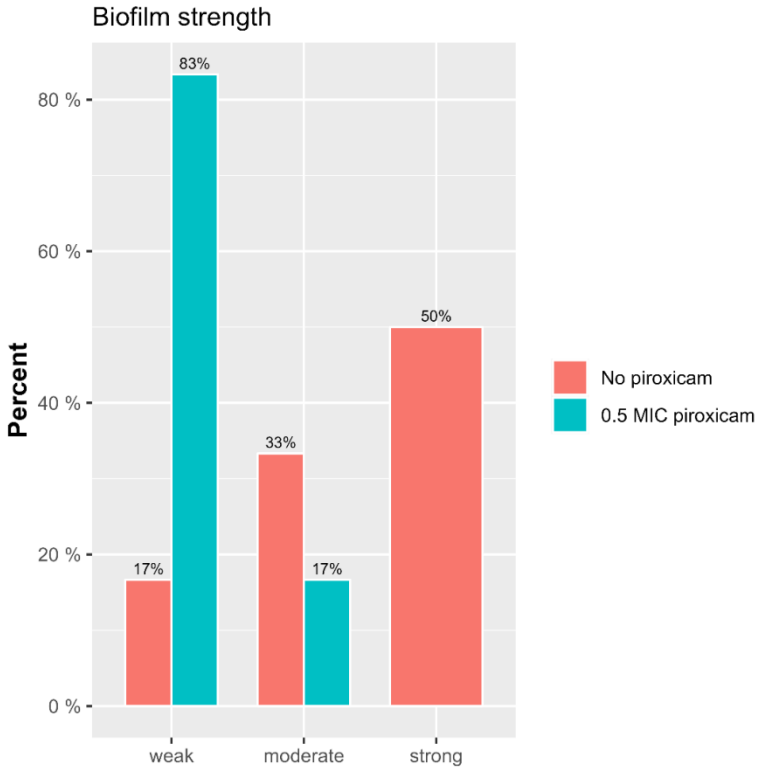

Figure 3. An overlay and binding pattern of B65 into active site (PDB 2ZCQ) 2D (A, C) and 3D (B, D) co-crystalized ligand (Brown), B65 (Green). An overlay and binding pattern of piroxicam into active site (PDB 2ZCQ) 2D (E, G) and 3D (F, H) Piroxicam (Red) and B65 (Brown).

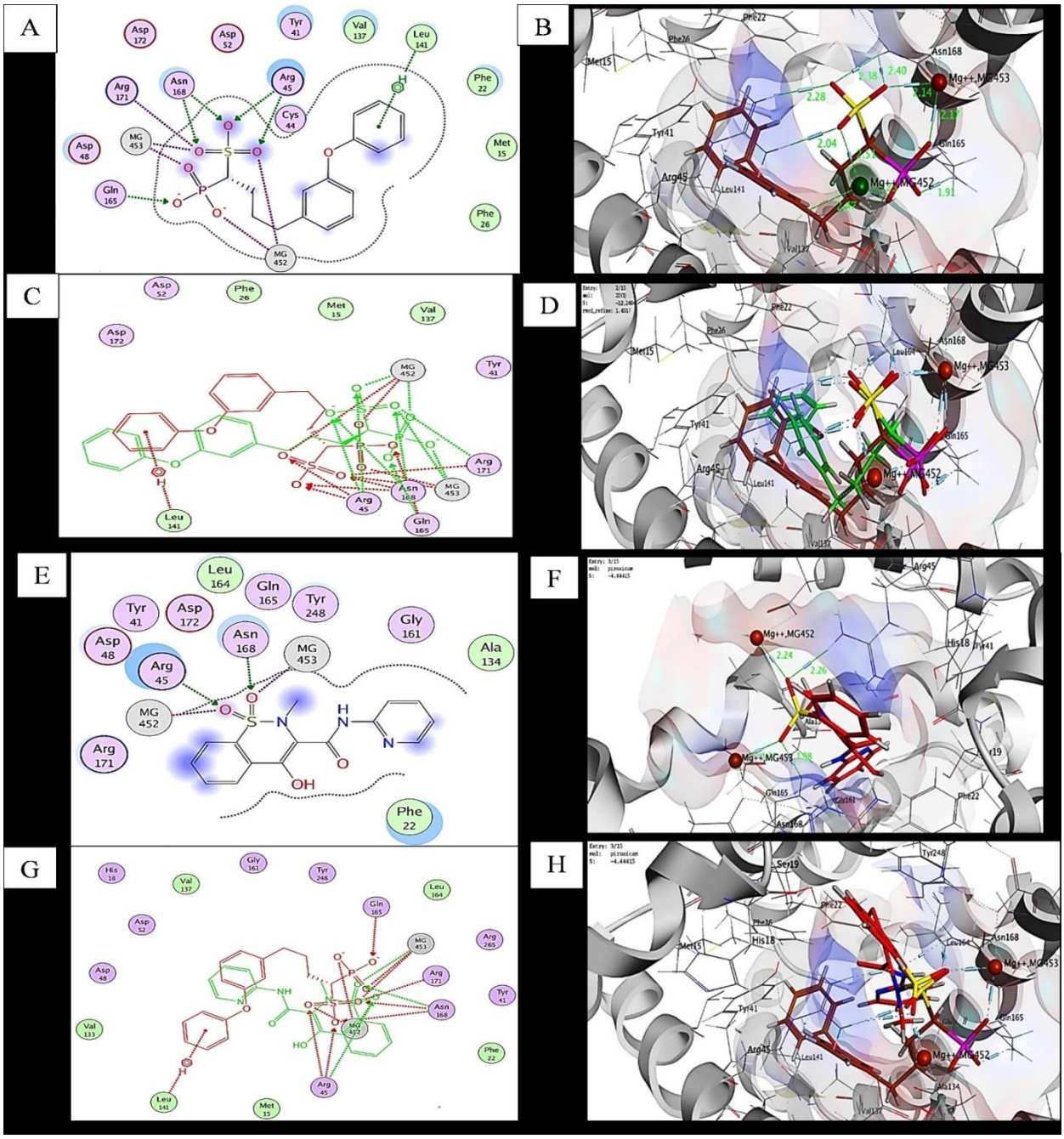

Figure 4. Binding pattern of piroxicam into active site (PDB 3GEU) 2D (A) and 3D (B). An overlay and binding pattern of piroxicam into active site (PDB 2KID) 2D (A, C) and 3D (B, D) co-crystalized ligand (Brown) and piroxicam (Red).

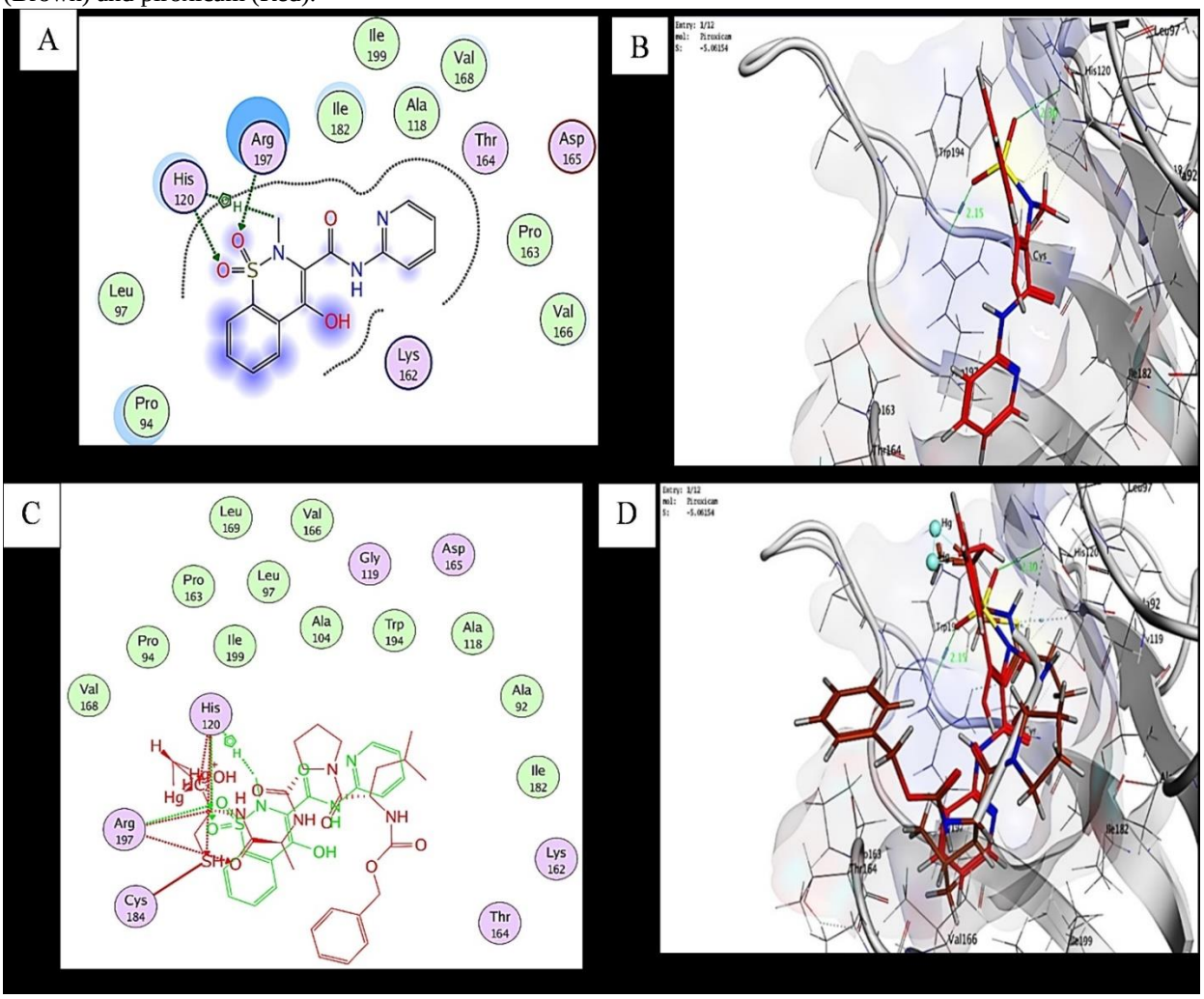

Figure 5. Binding pattern of piroxicam into active site (PDB 2VID) 2D (A) and 3D (B). Binding pattern of piroxicam into active site (PDB 7AHL) 2D (C) and 3D (D). Binding pattern of piroxicam into active site (PDB 3BS1) 2D (E) and 3D (F).

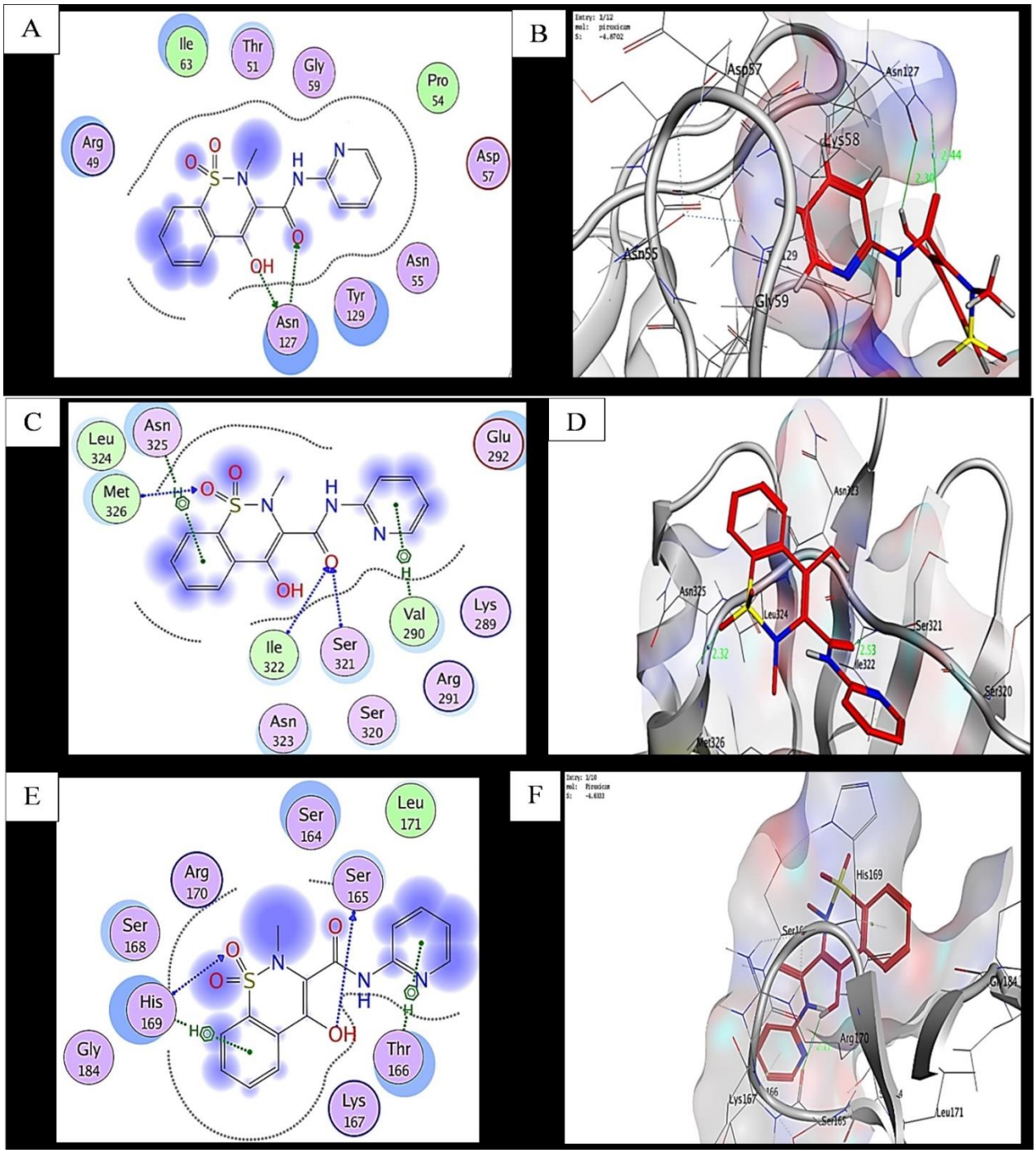

Discussion

Staphylococcus aureus is a human pathogen which causes many infections due variety of virulence factors [1]. In addition, biofilm formation provides a great treatment challenge due to higher antimicrobial resistance [4].

The uncontrollable increase of antimicrobial resistance poses a worldwide health hazard. MRSA is considered one of the significant clinical problems emerged mainly due to improper utilization of antibiotics [2]. One of the strategies proposed to counteract the antimicrobial resistance is the anti-virulence therapy [7], through repositioning of some FDA-approved drugs [8].

Therefore, this study aimed to repurpose piroxicam, an FDA- approved- NSAID- and asses its anti-virulence effect against MRSA clinical isolates.

Piroxicam MIC was first determined to estimate the sub-MIC for assessment of its anti-virulence activity and to exclude its effect on the bacterial cell's growth. Piroxicam showed MIC of 2.5 mg/ml for all the investigated isolates and was 1.25 mg/ml for the ATCC 25923 strain. Also, other studies reported the antibacterial effects of piroxicam. Leão et al stated that MIC of piroxicam was >2000 µg/ml for *S. aureus* [8]. Elshaer et al stated that MIC of piroxicam against *Acinetobacter baumannii* was 1.25-2.5 mg/ml [26].

We observed that piroxicam had a significant ani-virulence effect for the phenotypically detected virulence factors. It caused a significant reduction for protease activity, hemolysin activity and staphyloxanthin production.

Some studies estimated the effect of piroxicam as anti-virulence agent. Consistent with the findings of the current study, Elshaer et al reported the significant inhibitory effect of piroxicam for *Acinetobacter baumanii* QS-associated virulence factors including surface motility and biofilm formation [26]. In another study, it was reported that piroxicam helped elimination of biofilm mass of *S. aureus* and *E. coli* [8].

The *agr* typing of the isolates included in this study revealed that 53.3% of the isolates were *agr1*, and 46.7% were *agr3*. None of the isolates were *agr2*, *agr4* or *agr* non-typable. Moreover, the inhibitory effect of piroxicam for staphyloxanthin production was highly significant in isolates of *agr1* type. In an Egyptian study by Rezk et al found that the most prevalent *agr* types within their MRSA isolates were *agr1*(51.1%) and *agr3* (24%). Whereas *agr2*, *agr4 and agr* non-typable isolates were 12%, 2.4% and 10.4%, respectively [27]. Also, Nasirian et al reported the highest prevalence of *agr* types was *agr1* (52%) and *agr3* (34.2%) among the studied MRSA isolates [28].

More studies also reported that highest prevalence of *agr1* was in *S. aureus* isolates [29, 30]. Like this finding, Derakhshan et al neither detected *agr2* nor *agr4* but found that *agr3* was the most detected type (44.7%) [31].

The MRSA isolates of this study can be considered of high virulence, where most of the isolates showed a phenotypic detection of the tested virulence factors. (100% produced hemolysin and staplyloxanthin and 86.7% had positive protease activity). This suggests a correlation between high virulence and *agr1* and *agr3* types. Similarly, Derakhshan et al reported that high virulence profile among *agr* types 1 and 3, where isolates of *agr3* were more virulent than *agr1* [31]. Other studies also suggested the association between *agr* typing positivity and *S. aureus* virulence [30, 32]. According to the phenotypic results, molecular docking studies were applied to investigate if piroxicam can bind to *S. aureus* virulence proteins. The results revealed high docking scores which indicate an antagonistic effect of piroxicam for dehydrosqualene synthase (2ZCQ), hemolysin (7AHL), serine protease (2VID), sortase enzyme (2KID), and AgrA LytTR (3BS1). This is consistent with the phenotypic inhibitory effects of piroxicam against staphyloxanthin production, hemolysin activity and protease activity.

On the other hand, there was a high docking score produced with IcaR protein. This protein is a repressor i.e., a negative regulator for *ica* locus that mainly controls biofilm formation [33]. This suggests that piroxicam acts as agonist for IcaR protein and hence increases its inhibitory effect on *ica* locus. Besides, piroxicam is suggested to have an inhibitory effect of on sortase enzyme (2KID) which was proved to have role in host cell adhesion and biofilm formation [34]. Therefore, this may provide a suggestion for the mechanism of action of piroxicam as anti-biofilm agent. Still, more studies are required to prove the exact mechanism of piroxicam as an anti-virulence and anti-biofilm agents.

Moreover, *in silico* molecular docking proved another potential interaction of agrA with piroxicam. This postulates an inhibitory effect for the *agr*-QS system and hence negatively affects the coordinated expression of virulence factors and the dispersion of mature biofilm. Actually, there is a debate about the role of *agr*-QS system in biofilm formation. Some studies stated that *agr*-QS system inhibition is associated with stimulation of biofilm formation and dispersion [35-37]. Conversely, other studies support the suggestion of the current study, that targeting the *agr* system will promote biofilm inhibition and impairs its dispersion [38-40]. Therefore, other studies are required to prove exactly the molecular mechanism of *agr* QS on biofilm formation.

Unfortunately, the current study did not support the investigation of quorum sensing and virulence genes expression; due to a lack of funding. We recommend further research on the in-vivo activity of piroxicam, alone and also in combination with traditional antibiotics in one or more infection models. This research could potentially suggest the use of piroxicam as an adjuvant therapy for MRSA infection. However, this study does confirm the significant anti-virulence and anti-biofilm effects of piroxicam against MRSA isolates.

Conclusions

Piroxicam has an antibacterial effect against MRSA isolates. At sub-inhibitory concentration it had a significant anti-virulence effect. This was confirmed through the piroxicam–virulence proteins interactions proved by the *in silico* molecular docking. Therefore, we conclude that piroxicam can be repurposed as an anti-virulence agent against MRSA infection. However, more studies are required to fully explain the detailed molecular mechanism behind its action, besides in vivo studies.

Disclosures

Conflict of interest

The authors report no conflicts of interest

Financial disclosure

No funding was received for conducting the current study.

Authors contributions

Ingy Elsoudany, Conceptualization; Methodology; Validation, Writing original draft. Maged A. El Sawy, Molecular docking studies, Methodology; Validation, Writing original draft. Rasha Emad, Data curation, Visualization and Formal analysis, Writing original draft. Nancy Attia, Sample collection, Methodology, Validation, Writing original draft. All authors have approved the final article.

Ethics statement

The authors confirm that the ethical policies of the journal, as noted on the journal's author guidelines page, have been adhered to and the Medical Research Institute ethical review committee approval has been received with the following approval number E/C. S/N. R16/2023.

References

1- Lowy FD. Staphylococcus aureus infections. New England journal of medicine 1998;339(8):520-32.

2- Liu S, She P, Li Z, Li Y, Li L, Yang Y, et al. Antibacterial and antibiofilm efficacy of repurposing drug hexestrol against methicillin-resistant Staphylococcus aureus. International Journal of Medical Microbiology 2023;313(2):151578.

3- Gordon RJ, and Lowy FD. Pathogenesis of methicillin-resistant Staphylococcus aureus infection. Clinical infectious diseases 2008;46(Supplement_5):S350-S9.

4- Xue L, Chen YY, Yan Z, Lu W, Wan D, Zhu H. Staphyloxanthin: a potential target for antivirulence therapy. Infection and drug resistance 2019:2151-60.

5- Abbas HA, Atallah H, El-Sayed MA, El-Ganiny AM. Diclofenac mitigates virulence of multidrug-resistant Staphylococcus aureus. Arch Microbiol 2020;202(10):2751-60 DOI 10.1007/s00203-020-01992-y.

6- Gray B, Hall P, Gresham H. Targeting agr-and agr-like quorum sensing systems for development of common therapeutics to treat multiple gram-positive bacterial infections. Sensors 2013;13(4):5130-66.

7- Dehbanipour R, and Ghalavand Z. Anti-virulence therapeutic strategies against bacterial infections: recent advances. Germs 2022;12(2):262.

8- Leao C, Borges A, Simoes M. NSAIDs as a drug repurposing strategy for biofilm control. Antibiotics Basel 2020.

9- Tille P. Bailey & Scott's diagnostic microbiology-E-Book. London: Elsevier Health Sciences; 2015.

10- Clinical and Laboratory Standards Institute. Performance Standards for Antimicrobial

Susceptibility Testing. CLSI 2022, M100, 32nd ed USA.

11- Alcaraz E, Centrón D, Camicia G, Quiroga MP, Di Conza J, Passerini de Rossi B. Stenotrophomonas maltophilia phenotypic and genotypic features through 4-year cystic fibrosis lung colonization. J Med Microbiol 2021;70(1):001281 DOI 10.1099/jmm.0.001281.

12- Xiang H, Qiu JZ, Wang DC, Jiang YS, Xia LJ, Deng XM. Influence of magnolol on the secretion of alpha-toxin by Staphylococcus aureus. Molecules 2010;15(3):1679-89 DOI 10.3390/molecules15031679.

13- AL-Kazaz EJ, Melconian AK, Kandela NJJIJS. Extraction of Staphyloxanthin from Staphylococcus aureus isolated from clinical sources to determine its antibacterial activity against other bacteria. 2014;55:1823-32.

14- Stepanović S, Vuković D, Hola V, Bonaventura GD, Djukić S, Ćirković I, et al. Quantification of biofilm in microtiter plates: overview of testing conditions and practical recommendations for assessment of biofilm production by staphylococci. 2007;115(8):891-9.

15- Hassan A, Usman J, Kaleem F, Omair M, Khalid A, Iqbal M. Evaluation of different detection methods of biofilm formation in the clinical isolates. Braz J Infect Dis 2011;15(4):305-11.

16- Lopes LAA, Dos Santos Rodrigues JB, Magnani M, de Souza EL, de Siqueira-Júnior JP. Inhibitory effects of flavonoids on biofilm formation by Staphylococcus aureus that overexpresses efflux protein genes. Microb Pathog 2017;107:193-7 DOI 10.1016/j.micpath.2017.03.033.

17- Yang JL, Wang MS, Cheng AC, Pan KC, Li CF, Deng SX. A simple and rapid method for extracting bacterial DNA from intestinal microflora for ERIC-PCR detection. World J Gastroenterol 2008;14(18):2872-6 DOI 10.3748/wjg.14.2872.

18- Sun W, Chen H, Liu Y, Zhao C, Nichols WW, Chen M, et al. Prevalence and characterization of heterogeneous vancomycin-intermediate Staphylococcus aureus isolates from 14 cities in China. Antimicrob Agents Chemother 2009;53(9):3642-9 DOI 10.1128/aac.00206-09.

19- Liu CI, Liu GY, Song Y, Yin F, Hensler ME, Jeng WY, et al. A cholesterol biosynthesis inhibitor blocks Staphylococcus aureus virulence. Science 2008;319(5868):1391-4 DOI 10.1126/science.1153018.

20- Song L, Hobaugh MR, Shustak C, Cheley S, Bayley H, Gouaux JE. Structure of staphylococcal alpha-hemolysin, a heptameric transmembrane pore. Science 1996;274(5294):1859-66 DOI 10.1126/science.274.5294.1859.

21- Dubin G, Stec-Niemczyk J, Kisielewska M, Pustelny K, Popowicz GM, Bista M, et al. Enzymatic activity of the Staphylococcus aureus SplB serine protease is induced by substrates containing the sequence Trp-Glu-Leu-Gln. J Mol Biol 2008;379(2):343-56 DOI 10.1016/j.jmb.2008.03.059.

22- Suree N, Liew CK, Villareal VA, Thieu W, Fadeev EA, Clemens JJ, et al. The structure of the Staphylococcus aureus sortase-substrate complex reveals how the universally conserved LPXTG sorting signal is recognized. J Biol Chem 2009;284(36):24465-77 DOI 10.1074/jbc.M109.022624.

23- Sidote DJ, Barbieri CM, Wu T, Stock AM. Structure of the Staphylococcus aureus AgrA LytTR domain bound to DNA reveals a beta fold with an unusual mode of binding.

Structure 2008;16(5):727-35 DOI 10.1016/j.str.2008.02.011.

24- Srivastava SK, Rajasree K, Fasim A, Arakere G, Gopal B. Influence of the AgrC-AgrA complex on the response time of Staphylococcus aureus quorum sensing. J Bacteriol 2014;196(15):2876-88 DOI 10.1128/jb.01530-14.

25- Ritchie TJ, and Macdonald SJ. How drug-like are 'ugly' drugs: do drug-likeness metrics predict ADME behaviour in humans? Drug Discov Today 2014;19(4):489-95 DOI 10.1016/j.drudis.2014.01.007.

26- Elshaer SL, Shaldam MA, Shaaban MI. Ketoprofen, piroxicam and indomethacin-suppressed quorum sensing and virulence factors in Acinetobacter baumannii. J Appl Microbiol 2022;133(4):2182-97 DOI 10.1111/jam.15609.

27- Rezk S, Alqabbasi OS, Ghazal A, El Sherbini E, Metwally DESJM, Diseases I. Association between accessory gene regulator alleles, agr functionality and biofilm formation in MRSA and MSSA isolated from clinical and nasal carrier specimens. 2023;4(2):459-67.

28- Nasirian S, Saadatmand S, Goudarzi H, Goudarzi M, Azimi HJAoCID. Molecular investigation of methicillin-resistant Staphylococcus aureus strains recovered from the intensive care unit (ICU) based on toxin, adhesion genes and agr locus type analysis. 2018;13(2).

29- Javdan S, Narimani T, Shahini Shams Abadi M, Gholipour A. Agr typing of Staphylococcus aureus species isolated from clinical samples in training hospitals of Isfahan and Shahrekord. BMC Res Notes 2019;12(1):363 DOI 10.1186/s13104-019-4396-8.

30- Xu Y, Qian SY, Yao KH, Dong F, Song WQ, Sun C, et al. Clinical and molecular characteristics of Staphylococcus aureus isolated from Chinese children: association among the agr groups and genotypes, virulence genes and disease types. World J Pediatr 2021;17(2):180-8 DOI 10.1007/s12519-021-00421-4.

31- Derakhshan S, Navidinia M, Haghi F. Antibiotic susceptibility of human-associated Staphylococcus aureus and its relation to agr typing, virulence genes, and biofilm formation. BMC Infect Dis 2021;21(1):627 DOI 10.1186/s12879-021-06307-0.

32- Zhang Y, Xu D, Shi L, Cai R, Li C, Yan H. Association Between agr Type, Virulence Factors, Biofilm Formation and Antibiotic Resistance of Staphylococcus aureus Isolates From Pork Production. Front Microbiol 2018;9:1876 DOI 10.3389/fmicb.2018.01876.

33- Jefferson KK, Pier DB, Goldmann DA, Pier GB. The teicoplanin-associated locus regulator (TcaR) and the intercellular adhesin locus regulator (IcaR) are transcriptional inhibitors of the ica locus in Staphylococcus aureus. J Bacteriol 2004;186(8):2449-56 DOI 10.1128/jb.186.8.2449-2456.2004.

34- Selvaraj C, Priya RB, Singh SK. Exploring the Biology and Structural Architecture of Sortase Role on Biofilm Formation in Gram Positive Pathogens. Curr Top Med Chem 2018;18(29):2462-80 DOI 10.2174/1568026619666181130133916.

35- He L, Le KY, Khan BA, Nguyen TH, Hunt RL, Bae JS, et al. Resistance to leukocytes ties benefits of quorum sensing dysfunctionality to biofilm infection. Nat Microbiol 2019;4(7):1114-9 DOI 10.1038/s41564-019-0413-x.

36- Suligoy CM, Lattar SM, Noto Llana M, González CD, Alvarez LP, Robinson DA, et al. Mutation of Agr Is Associated with the

Adaptation of Staphylococcus aureus to the Host during Chronic Osteomyelitis. Front Cell Infect Microbiol 2018;8:18 DOI 10.3389/fcimb.2018.00018.

37- Ford CA, Hurford IM, Cassat JE. Antivirulence Strategies for the Treatment of Staphylococcus aureus Infections: A Mini Review. Front Microbiol 2020;11:632706 DOI 10.3389/fmicb.2020.632706.

38- Dotto C, Lombarte Serrat A, Ledesma M, Vay C, Ehling-Schulz M, Sordelli DO, et al. Salicylic acid stabilizes Staphylococcus aureus biofilm by impairing the agr quorum-sensing system. Sci Rep 2021;11(1):2953 DOI 10.1038/s41598-021-82308-y.

39- Boles BR, and Horswill ARJPp. Agr-mediated dispersal of Staphylococcus aureus biofilms. 2008;4(4): e1000052.

40- Jenul C, and Horswill AR. Regulation of Staphylococcus aureus Virulence. Microbiol Spectr 2019;7(2)DOI 10.1128/microbiolspec.GPP3-0031-201

El-Soudany I, Elsawy MA, Emad R, Attia N. Piroxicam repurposing approach as an anti-virulence agent against methicillin resistant *Staphylococcus aureus* clinical isolates. Microbes Infect Dis 2024; 5(2): 632-646.